Sensorless Control of PMSM using FOC Strategy Based on Multiple ANN and Load Torque Observer

Marcel NICOLA[1]
[1]Research Department
National Institute for Research, Development and Testing in Electrical Engineering – ICMET
Craiova, Romania
marcel_nicola@yahoo.com

Claudiu-Ionel NICOLA[1,2], Marian DUȚĂ[1]
[2]Department of Automatic Control and Electronics
University of Craiova
Craiova, Romania
claudiu@automation.ucv.ro, marianduta@icmet.ro

***Abstract*—This article presents the sensorless control system of a Permanent Magnet Synchronous Motor (PMSM), where the speed controller consists of a Mutliple - Artificial Neural Networks (M-ANN) and the rotor speed is provided by a Sliding Mode Observer (SMO). The performance of the proposed control system is presented in comparison with the classic Field Oriented Control (FOC) system. The implementation of a load torque observer allows the selection of a specially trained corresponding ANN to obtain optimum performance over the load torque variation ranges. The PMSM equations, the speed and load torque observers equations, the main blocks and control structures, their parameterizations and the results of the numerical simulations obtained are presented. The good results obtained as a result of the numerical simulations involving the use of the usual Simulink and Stateflow blocks, which can be implemented in embedded systems recommend the real-time implementation of the proposed PMSM control system.**

Keywords—State observers; Artificial neural networks; Motor drives; Permanenet magnet motors; Automatic control

I. INTRODUCTION

It is undeniable that there has been a growing interest in the PMSM lately. This is explained by the fact that the PMSM has a number of advantages over other types of motors: low inertia, high load torque density, reduced dimensions, but also faster cooling, considering that the losses are concentrated in the stator and the harmonic content is lower [1-4].

Naturally, a series of PMSM control systems have been developed. Thus, we can mention the classic FOC and Direct Torque Control (DTC) control structures, but also modern adaptive, robust and predictive type control structures [5-8]. The intelligent PMSM control can be achieved by using fuzzy, ANN, genetic or Particle Swarm Optimization (PSO) type control algorithms [9, 10]. In order to eliminate the disadvantages of using position and speed transducers, a number of estimators were achieved, among which we can mention: estimators based on the SMO method, Model Reference Adaptive System (MRAS) and Luenberger observer for the deterministic approach and Kalman-type estimators for a stochastic type approach [11-14]. It is obvious that the deterministic estimators have the advantage of reduced complexity relative to the stochastic ones, but they have lower accuracy as compared to them.

A particular role in the modern control systems is given by their implementation using the ANN [15-17]. Among the main advantages of the ANN we can mention the robustness and the implementation of very complex systems by simply knowing the evolution in time of their input and output. This article presents the sensorless control system of a PMSM using a M-ANN for the speed control, a load torque estimator and a SMO-type rotor speed and position estimator. The load torque can be considered from the point of view of the PMSM automatic control system as disturbance parameter. Thus, a key element in the overall control structure proposed in this article is the presence of a load torque estimator. By knowing the range of the usual load torque variation, a number of ANNs will be trained on significant intervals, depending on the application, to reproduce the control achieved with FOC-type structure with PI-type controllers tuned for each of these sub-intervals of the load torque variation. By selecting the corresponding ANN, according to the estimated value of the load torque, superior performances will be achieved compared to the use of a FOC structure by tuning the control parameters for the entire range of the load torque variation. The rest of the paper is organized as follows: Section II describes the mathematical model of the PMSM and the FOC-type control structure. The mathematical models and the structures of implementation of the speed and load torque estimators in the Matlab/Simulink environment are presented in Section III. Section IV presents the ANN structures which selectively perform the PMSM control, based on the estimated load torque, and the results of the numerical simulations. The final section summarizes the conclusions and ideas for the continuation of the topics addressed in this article.

II. PMSM AND FOC STRATEGY - MATHEMATICAL MODEL

By using the usual notations in the rotor reference frame and by following [3, 17], the mathematical model of the PMSM in d-q frame can be written as follows:

$$\begin{bmatrix} u_q \\ u_d \end{bmatrix} = \begin{bmatrix} R_q + \rho L_q & \omega_e L_d \\ -\omega_e L_q & R_d + \rho L_d \end{bmatrix} \begin{bmatrix} i_q \\ i_d \end{bmatrix} + \begin{bmatrix} \omega_e \lambda_0 \\ \rho \lambda_0 \end{bmatrix} \quad (1)$$

This paper was developed with funds from the Ministry of Research and Innovation as part of the NUCLEU Program: PN 19 38 01 03.

978-1-7281-6870-8/20/$31.00 ©2020 IEEE

where: R_q, R_d and L_q, L_d are the stator resistances and inductances in the d-q reference frame of the PMSM, ω_e is the electrical angular velocity of the rotor, λ_0 represents the flux linkage, ρ is the differential operator, while i_d, i_q and u_d, u_q are the stator voltages and currents in the d-q reference frame.

The flux on the d-q axes are given by:

$$\begin{aligned} \lambda_q &= L_q i_q \\ \lambda_d &= L_d i_d + \lambda_0 \end{aligned} \tag{2}$$

By indicating the electromagnetic torque developed by the PMSM as T_e the following relations regarding the PMSM dynamics can be expressed:

$$\begin{aligned} T_e &= \frac{3}{2} n_p \left\{ \lambda_d i_q - \lambda_q i_d \right\} \\ T_e &= T_L + B\omega + J\frac{d\omega}{dt} \end{aligned} \tag{3}$$

where: n_p is the number of pole pairs, B is the viscous friction coefficient, J is the rotor inertia and T_L is the load torque.

If we consider the simplifications $L_d=L_q=L$, $R_d=R_q=R_s$, and $\omega_e=n_p \cdot \omega$ where ω is the angular velocity of the rotor, then the PMSM model becomes:

$$\begin{pmatrix} \dot{i}_d \\ \dot{i}_q \\ \dot{\omega} \end{pmatrix} = \begin{pmatrix} -\frac{R_s}{L} & n_p\omega & 0 \\ -n_p\omega & -\frac{R_s}{L} & -\frac{n_p\lambda_0}{L} \\ 0 & \frac{K_t}{J} & -\frac{B}{J} \end{pmatrix} \begin{pmatrix} i_d \\ i_q \\ \omega \end{pmatrix} + \begin{pmatrix} \frac{u_d}{L} \\ \frac{u_q}{L} \\ -\frac{T_L}{J} \end{pmatrix} \tag{4}$$

where: K_t is the torque constant.

The classic FOC-type control structure of the PMSM is shown in Fig. 1 [3]. The FOC-type control structure shown in Fig. 1 contains a cascade control system where the outer loop is intended for the control the rotor speed of the PMSM motor. The current reference i_d is set to zero for torque maximization reasons, and the reference i_q for the inner current control loop is prescribed by the PI-type speed controller. The SVPWM (Space Vector Pulse Width Modulation) block ensures the transition of the IGBTs (power transistors) according to the control inputs u_α and u_β and a switching table [3].

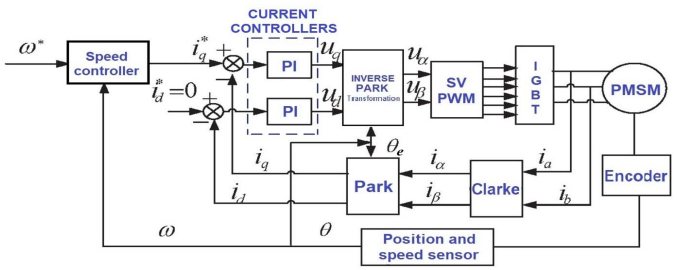

Fig. 1. Block diagram of the FOC strategy for the PMSM

III. Rotor Speed and Load Torque Estimation

The speed estimator equations are obtained based on the PMSM model given by equations (1)-(4), and by using the transformation matrix in (5), the equations in the α-β frame (using Park inverse transformation) are obtained.

$$T = \begin{pmatrix} \cos\theta_e & -\sin\theta_e \\ \sin\theta_e & \cos\theta_e \end{pmatrix} \tag{5}$$

Based on these, the currents i_α, i_β and the back-EMF e_α and e_β are given by the relations (6) and (7) respectively:

$$\begin{aligned} i_\alpha &= i_d \cos(\theta_e) - i_q \sin(\theta_e) \\ i_\beta &= i_d \sin(\theta_e) + i_q \cos(\theta_e) \end{aligned} \tag{6}$$

$$\begin{aligned} e_\alpha &= \frac{d\lambda_\alpha}{dt} = -\lambda_0 \omega_e \sin(\theta_e) \\ e_\beta &= \frac{d\lambda_\beta}{dt} = -\lambda_0 \omega_e \cos(\theta_e) \end{aligned} \tag{7}$$

In the α-β frame, the PMSM equations can be synthetized as in the following relation:

$$\begin{aligned} \frac{di_\alpha}{dt} &= -\frac{R_s}{L} i_\alpha - \frac{1}{L} e_\alpha + \frac{1}{L} u_\alpha \\ \frac{di_\beta}{dt} &= -\frac{R_s}{L} i_\beta - \frac{1}{L} e_\beta + \frac{1}{L} u_\beta \end{aligned} \tag{8}$$

By estimating the back-EMF e_α and e_β, by using a SMO, the position and the speed of the rotor can then be estimated. The equations of the observer are given in the following relation [17]:

$$\begin{aligned} \frac{d\hat{i}_\alpha}{dt} &= -\frac{R_s}{L}\hat{i}_\alpha + \frac{1}{L}u_\alpha - \frac{1}{L}kH(\hat{i}_\alpha - i_\alpha) \\ \frac{d\hat{i}_\beta}{dt} &= -\frac{R_s}{L}\hat{i}_\beta + \frac{1}{L}u_\beta - \frac{1}{L}kH(\hat{i}_\beta - i_\beta) \end{aligned} \tag{9}$$

where: k is the observer gain, and function H is of the sigmoid type:

$$H(x-y) = \frac{2}{1+e^{-a(x-y)}} - 1 \tag{10}$$

where: a is a positive constant, and the sigmoid function defined by (10) will take values between -1 and 1 for a=4 and will replace the *sign* function of the classic approach of the SMO, resulting in the reduction of the chattering phenomenon.

The sliding vector is defined as:

$$S_n = [s_\alpha \; s_\beta]^T = [\hat{i}_\alpha - i_\alpha \; \hat{i}_\beta - i_\beta]^T = [\bar{i}_\alpha \; \bar{i}_\beta]^T \quad (11)$$

and Lyapunov function is chosen as follows [17]:

$$V = \frac{1}{2} S_n^T S_n = \frac{1}{2}\left(s_\alpha^2 + s_\beta^2\right) \quad (12)$$

Parameter k is chosen such that $\dot{V} < 0$, ensuring the SMO stability when the system trajectory is on the sliding surface, S_n=0. The system of equations of the errors of currents is defined as follows:

$$\begin{aligned} \dot{\bar{i}}_\alpha &= \dot{\hat{i}}_\alpha - \dot{i}_\alpha = -\frac{R_s}{L}\bar{i}_\alpha + \frac{1}{L}e_\alpha - \frac{1}{L}kH(\bar{i}_\alpha) \\ \dot{\bar{i}}_\beta &= \dot{\hat{i}}_\beta - \dot{i}_\beta = -\frac{R_s}{L}\bar{i}_\beta + \frac{1}{L}e_\beta - \frac{1}{L}kH(\bar{i}_\beta) \end{aligned} \quad (13)$$

By calculating $\dot{V}$, the following relation is obtained [17]:

$$\dot{V} = -\frac{R_s}{L}\left(\bar{i}_\alpha^2 + \bar{i}_\beta^2\right) + \frac{1}{L}\left[\left(e_\alpha - k\right)\bar{i}_\alpha H(\bar{i}_\alpha) + \left(e_\beta - k\right)\bar{i}_\beta H(\bar{i}_\beta)\right] < 0 \quad (14)$$

And to fulfill the condition $\dot{V} < 0$, the observer gain is chosen as follows:

$$k \geq \max\left(\left|e_\alpha\right|, \left|e_\beta\right|\right) \quad (15)$$

The sliding mode is obtained on the surface:

$$[\dot{s}_\alpha \; \dot{s}_\beta]^T = [s_\alpha \; s_\beta]^T \approx [0 \; 0] \quad (16)$$

Thus, from the relations (14)-(16), the estimates for the back-EMF e_α and e_β are obtained in the following form:

$$\begin{aligned} \hat{e}_\alpha &= kH(\bar{i}_\alpha) = -\lambda_0 \hat{\omega}_e \sin\theta_e \\ \hat{e}_\beta &= kH(\bar{i}_\beta) = \lambda_0 \hat{\omega}_e \cos\theta_e \end{aligned} \quad (17)$$

The rotor speed and position estimates can be obtained from the relation (17), in the form of the following relations:

$$\hat{\omega}_e = \frac{\sqrt{\hat{e}_\alpha^2 + \hat{e}_\beta^2}}{\lambda_0} \quad (18)$$

$$\hat{\theta}_e(t) = \int_{t_0}^{t} \hat{\omega}_e(t)dt + \theta_0 \quad (19)$$

where: θ_0 is the initial electrical position of the rotor.

The implementation of the speed observer in Matlab/Simulink is shown in Fig. 2. The equations (9) describing the observer are implemented as the subsystem on the left side of the block diagram in Fig 2. The sigmoid function is used, instead of the sign function, to smooth the inherent oscillations in a SMO. In the final part of the SMO implementation, an intermediate filter block of the back-EMF e_α and e_β is also added as low-pass filters with a cut-off frequency of 500Hz.

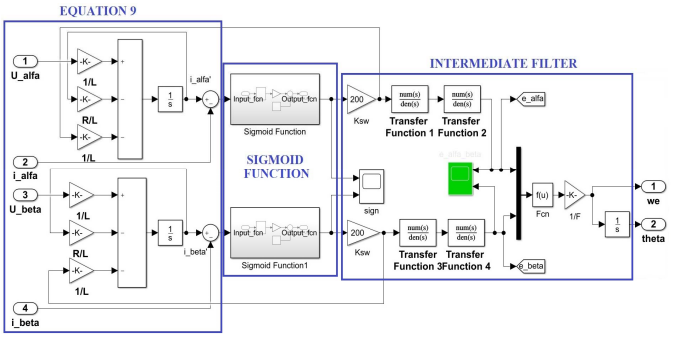

Fig. 2. Block diagram of rotor speed and position SMO implementation in Matlab/Simulink

Fig. 3 presents the results of the numerical simulations of the evolution in time of quantities provided by the SMO: rotor speed and position, back-EMF e_α and e_β and further i_d and i_q currents. A very good estimation of the parameters provided by the SMO is noticed. For constructive reasons, the PMSM has a special start, so that up to 100ms the operation is done in the open loop, after a predefined current sequence. For this reason, the rotor speed is not estimated during this time period. The nominal parameters of the PMSM are given in Table I.

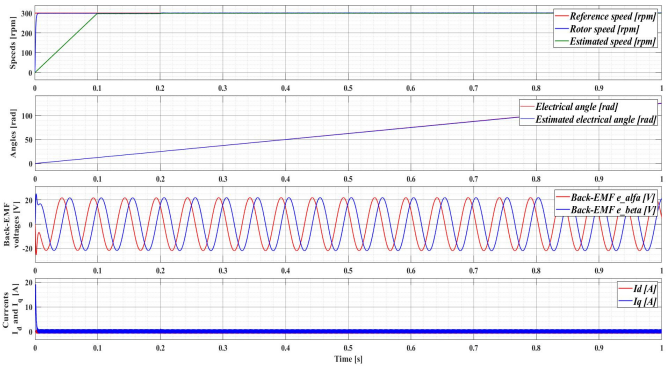

Fig. 3. Simulation of the back-EMF, rotor position and rotor speed time evolution from the SMO

The relations (3) are used for the estimation of the load torque, and the implementation in Matlab/Simulink is presented in the block diagram in Fig. 4. On the left side of the block diagram there is a subsystem which implements the relations (3), and on the right side there is a block of adjustment of the output to get a good estimate of the load torque. Fig. 5 shows the results of the numerical simulations of the evolution in time of the load torque estimate for a prescribed sequence of the following form: [0.1 0.25 0.5 0.75 1 1.25]s→[1 2 3 4 3 3 2]Nm (to which a uniformly distributed noise with an amplitude of 0.4Nm is added).

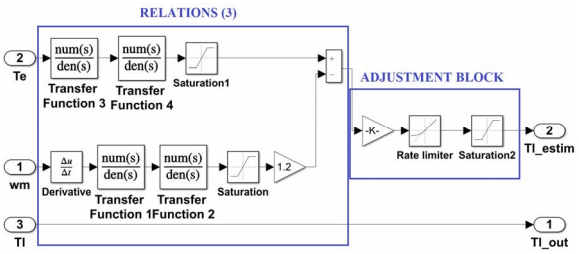

Fig. 4. Block diagram of the load torque observer implementation in Matlab/Simulink

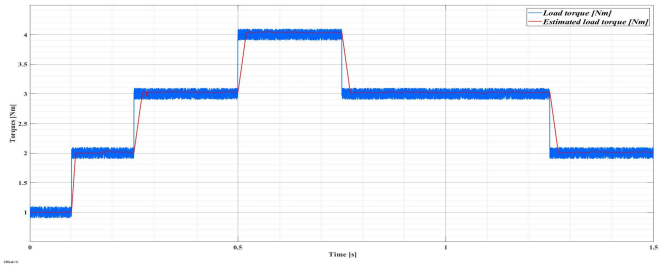

Fig. 5. Time evolution simulation of the estimated load torque

IV. Sensorless Control of the PMSM Using Multiple ANN – Numerical Simulation

The PMSM control system proposed in this article replaces the PI-type speed controller in the FOC-type structure presented in Section II, with a control system based on a series of ANNs (see Fig. 6), selected according to the load torque value. In the electric drives, the load torque is an external signal, considered as a disturbance from the point of view of the speed control system, so that it is imperative to use a load torque observer T_L. Also, since the control system is sensorless, a rotor speed observer will be used as presented in Section III. Depending on the application, the load torque variation range is divided into sub-intervals, and on each of these sub-intervals, the speed controller is optimally tuned and the speed error values (the PI-type speed controller input) and i_{q_ref} (the PI-type speed controller output) are saved as two vectors. After this stage, each ANN is trained with these vectors. Depending on the load torque value (provided by the observer), the specially trained ANN is selected, obtaining superior performance over a classic FOC structure, where the PI-type speed controller performs the speed control over the entire range of the speed reference and load torque.

The numerical simulations were performed in the Matlab/Simulink environment. The implementation of the ANN selection according to the load torque is presented in Fig. 7. The implementation is based on the Stateflow toolbox in Matlab.

The PI type controller has the transfer function:

$$H_{PI}(s) = K_p + K_i \frac{1}{s} \tag{20}$$

For discretization, the Tustin substitution of the following form is used:

$$s = \frac{2}{T_s}\frac{z-1}{z+1} \tag{21}$$

The sampling period T_s used in the Matlab/Simulink numerical simulations is of 2μs. In Equations (20) and (21), the continuous and discrete variables are denoted as s and z respectively.

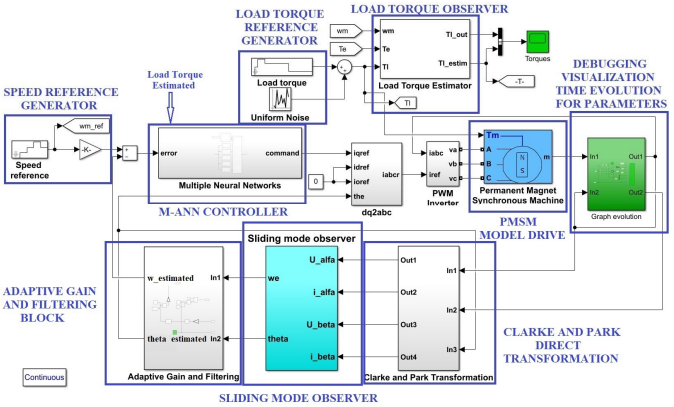

Fig. 6. Sensorless control of the PMSM based on M-ANN using rotor speed SMO and load torque observer

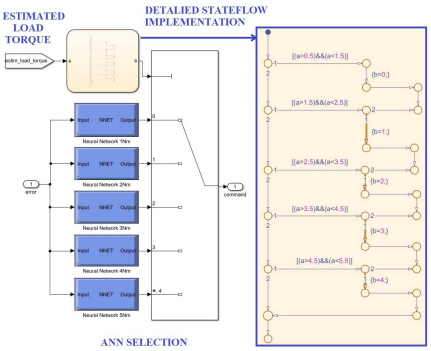

Fig. 7. Simulink subsystem for the selection of the ANN

The block diagram of an ANN structure is presented in Fig. 8. The Deep Learning toolbox was used for the implementation of the ANN in Matlab. The selected ANN is of the Neural Fitting type with two Layers (Hidden Layer with 150 neurons and Output Layer with 1 neuron). For the training of each ANN, the sample length of the input/output vectors (the input/output of the PI-type speed controller) is of 125224 samples. Of these, 87565 samples were used for training, 18784 samples for validation and 18784 samples for testing. The Levenberg-Marquardt method was chosen for the training process of each ANN.

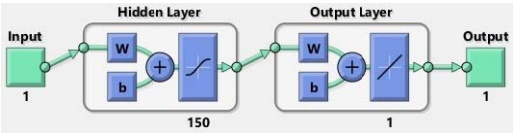

Fig. 8. Block diagram of the ANN structure

The performance of the training of an ANN corresponding to a sub-interval of the load torque is presented in Fig. 9 and

10. The value close to 1 of the regression parameter R in Fig. 9 (which represents a measure of the approximation between output and target) is a guarantee that the ANN has been successfully trained.

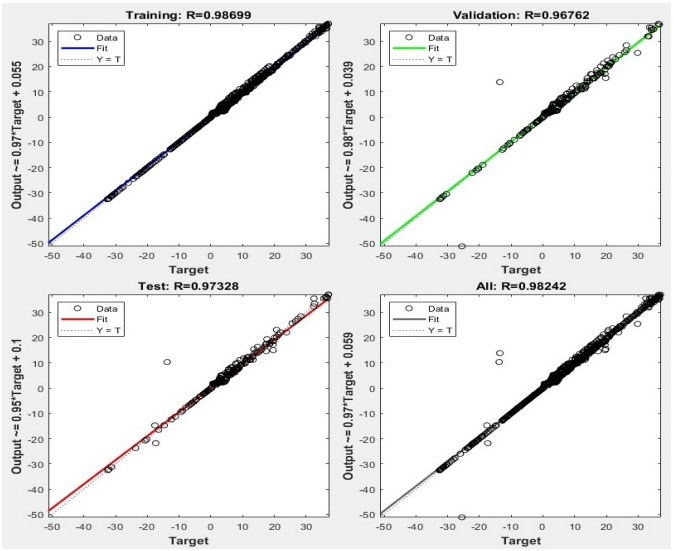

Fig. 9. Regression R – after the training of the ANN

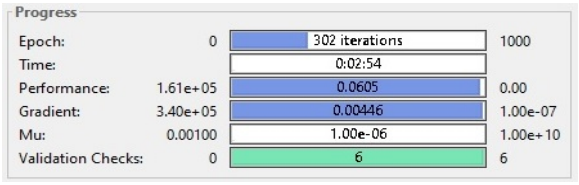

Fig. 10. Training state of the ANN - performance

For the numerical simulation in the Matlab/Simulink environment, a PMSM with the nominal parameters given in Table I was selected.

TABLE I. PMSM - NOMINAL PARAMETERS

Parameter	Value	Unit
Stator resistance - R_s	2.875	Ω
q and d inductance - L_q and L_d	0.0085	H
Combined inertia of rotor and load - J	0.8e-3	kg·m^2
Combined viscous friction of rotor and load - B	0.005	N·m·s/rad
Flux induced by the permanent magnets of the rotor in the stator phases - λ_0	0.175	Wb
Pole pairs number - P	4	-

In Fig. 11-14, the speed profile required to compare the performance of the M-ANN-based control systems to the FOC-type control system is described by the following sequence: [0 0.25 0.5 0.75 1 1.25]s→[300 600 900 1200 900 600]rpm. For PMSM used in the numerical simulations, the nominal load torque is of 3Nm. For a load torque profile with a relatively low dynamic described by the sequence: [0 0.25 0.5 0.75 1.25]s→[1 2 3 3 2]Nm (to which a uniformly distributed noise with an amplitude of 0.4Nm is added), after an optimal tuning of the PI-type speed controller (using the Ziegler-Nichols tuning method), a good response is obtained like the one in Fig. 11. If the load torque has a dynamic given by the sequence: [0 0.05 0.1 0.25 0.5 0.75 1 1.25]s→[1 3 5 4 4 2 2 3]Nm, to which a uniformly distributed noise of the type described above is added, the best tuning of the PI controller provides the results obtained in Fig. 12. It can be observed that the profile cannot be tracked with good results in the 0-100ms range when the load torque has a fast variation, but also shortly after the 750ms time, when the load torque has a relatively high value at a speed of 1200rpm. By selecting five equal sub-intervals of the load torque variation, 5 ANNs were trained under the conditions in which the optimal tunings of the PI-type speed controller were achieved for each of these sub-intervals. In this way, it can be seen in Fig. 13 that higher performance was obtained compared to a PI controller tuned for the entire load torque variation range. The value of the speed ripple is defined as follows [5]:

$$\omega_{rip} = \sqrt{\frac{1}{N}\sum_{i=1}^{N}\left(\omega(i) - \omega_{ref}(i)\right)^2} \tag{22}$$

where: N represents the number of samples, ω and ω_{ref} represent the rotor speed and respectively, the prescribed reference of speed.

By calculating the speed ripple for the system response in Fig. 12, a value of 16.273rpm is obtained. Using the M-ANN based controller for the same speed and load torque profile defined above, a reduction of the speed ripple by approximately 25% is obtained.

Also, the speed profile is tracked with good fidelity by the M-ANN based controller in the areas specified above where the classic controller provided modest results. Regarding the parametric robustness of the M-ANN-based controller in Fig. 14, the results of the numerical simulation for the speed and load torque profiles described above are presented, under the conditions where the J parameter (combined inertia of rotor and load) has a 50% increase (from 0.8e-3 kg·m^2 to 1.2e-3 kg·m^2). A good response of the M-ANN-based control is also noticed in the case of the parametric variation.

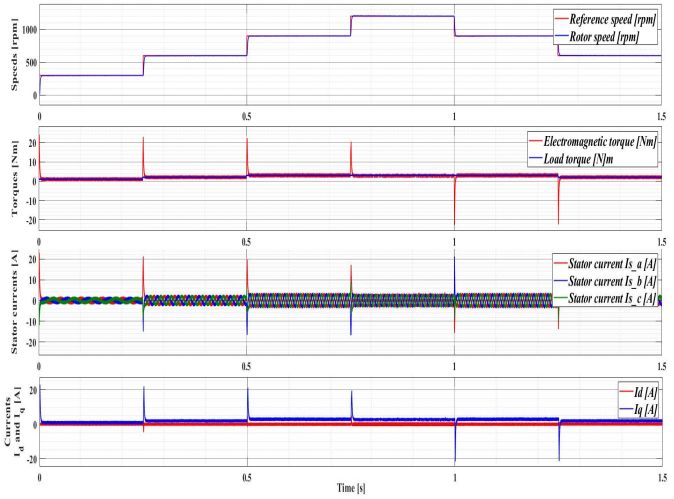

Fig. 11. Simulation of the PMSM time evolution with FOC strategy and low/medium variation of the load torque

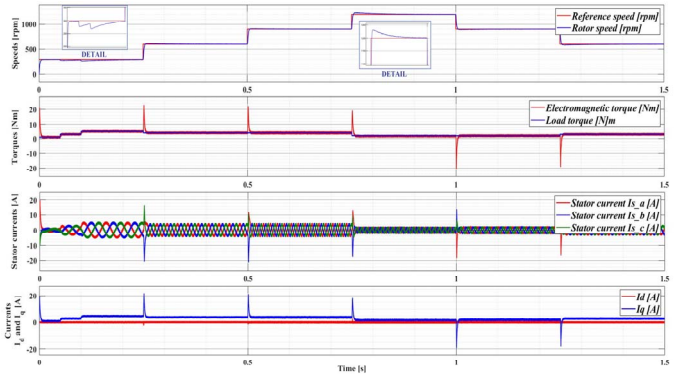

Fig. 12. Simulation of the PMSM time evolution with FOC strategy and high variation of the load torque

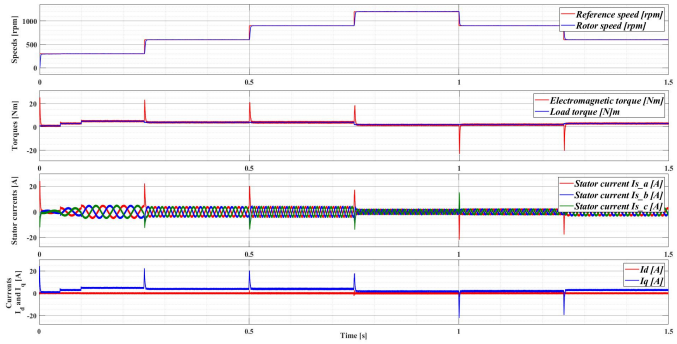

Fig. 13. Simulation of the PMSM time evolution with M-ANN and high variation of the load torque

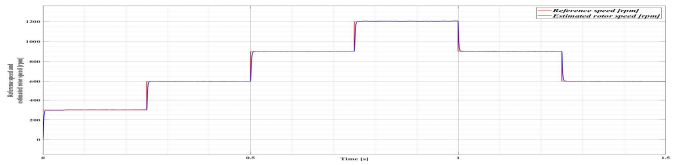

Fig. 14. Simulation of the PMSM time evolution with M-ANN and high variation of the load torque and 50% increase of J parameter

V. CONCLUSIONS

This article presents the sensorless control system of a PMSM, where the speed controller consists of a M-ANN, the rotor speed is provided by a SMO-type observer, and better performances was obtained compared to the classic FOC-type control system based on PI-type speed controller. A key element is the implementation of a load torque observer, which allows the selection of a specially trained corresponding ANN for optimum performance over the load torque variation ranges. The PSMS equations, the speed and load torque observers equations, the main blocks and control structures, and the results of the numerical simulations obtained are also presented. Following the good results obtained from the numerical simulations and the use of the usual Simulink and Stateflow blocks (which can be implemented in embedded systems), future approaches will present the real-time implementations of the control system of the proposed PMSM using hardware dedicated platforms with DSP controllers.

REFERENCES

[1] V. Utkin, J. Guldner, J. Shi, Sliding mode control in electromechanical systems, second edition. Automation and Control Engineering, Taylor & Francis, 2009.

[2] Y. Zhao, "Position/speed sensorless control for permanent-magnet synchronous machines," Ph.D. dissertation, Electrical Engineering, Univ. Nebraska – Lincoln, Lincoln, 2014.

[3] B. K. Bose, Modern power electronics and AC drives, Prentice Hall, Knoxville, Tennessee, USA, 2002.

[4] S. Hussain and M. A. Bazaz, "Comparative analysis of speed control strategies for vector controlled PMSM drive," *International Conference on Computing, Communication and Automation (ICCCA)*, Noida, India, 2016, pp. 1314-1319.

[5] B. Ning, S. Cheng, and Y. Qin, "Direct torque control of PMSM using sliding mode backstepping control with extended state observer," in Journal of Vibration and Control , vol. 24, no.4, pp. 694-707, Feb. 2018.

[6] P. M. Nicolae, M. C. Nitu and D. Constantin, "Direct flux vector control for dual-three phase induction motor drives," *4th International Youth Conference on Energy (IYCE)*, Siofok, Hungary, 2013, pp. 1-5.

[7] C. Nicola, M. Nicola, S. Popescu, and M. Duţă, "Power Factor Correction and Sensorless Control of PMSM Using FOC Strategy," *International Conference on Electromechanical and Energy Systems (SIELMEN)*, Craiova, Romania, 2019, pp. 1-6.

[8] M. Nicola and C. Nicola, "Sensorless Predictive Control for PMSM Using MRAS Observer," *International Conference on Electromechanical and Energy Systems (SIELMEN)*, Craiova, Romania, 2019, pp. 1-7.

[9] M. Mutluer and O. Bilgin, "Design optimization of PMSM by particle swarm optimization and genetic algorithm," *12 International Symposium on Innovations in Intelligent Systems and Applications*, Trabzon, Turkey, 2012, pp. 1-4.

[10] W. A. A. Salem, G. F. Osman, and S. H. Arfa, "Adaptive Neuro-Fuzzy Inference System Based Field Oriented Control of PMSM & Speed Estimation," *Twentieth International Middle East Power Systems Conference (MEPCON)*, Cairo, Egypt, 2018, pp. 626-631.

[11] K. Kyslan, V. Šlapák, V. Fedák, F. Ďurovský, and K. Horváth, "Design of load torque and mechanical speed estimator of PMSM with unscented Kalman filter - An engineering guide," *19th International Conference on Electrical Drives and Power Electronics (EDPE)*, Dubrovnik, Croatia, 2017, pp. 297-302.

[12] N. Henwood, J. Malaizé and L. Praly, "A robust nonlinear Luenberger observer for the sensorless control of SM-PMSM: Rotor position and magnets flux estimation," *38th Annual Conference on IEEE Industrial Electronics Society (IECON)*, Montreal, Canada 2012, pp. 1625-1630.

[13] A. Aissa, K. Ameur, and B. Mokhtari, "MRAS for Speed Sensorless Direct Torque Control of a PMSM Drive Based on PI Fuzzy Logic and Stator Resistance Estimator," in Transaction on Control and Mechanical Systems, vol. 2, no. 7, pp. 321-326, Jul. 2013.

[14] B. Liu, "Speed control for permanent magnet synchronous motor based on an improved extended state observer," in Advances in Mechanical Engineering, vol. 10, no.1, pp. 1-12, Nov. 2018.

[15] S. K. Suman, M. K. Gautam, R. Srivastava and V. K. Giri, "Novel approach of speed control of PMSM drive using neural network controller," *International Conference on Electrical, Electronics, and Optimization Techniques (ICEEOT)*, Chennai, China, 2016, pp. 2780-2783.

[16] J. Lee and J. Ha, "On-Line Switch-Open Fault Detection of PMSM Using Artificial Neural Network," *10th International Conference on Power Electronics and ECCE Asia (ICPE 2019 - ECCE Asia)*, Busan, Korea (South), 2019, pp. 1-6.

[17] M. S. Wang and T. M. Tsai, "Sliding Mode and Neural Network Control of Sensorless PMSM Controlled System for Power Consumption and Performance Improvement," in Energies, vol. 10, no. 11, pp. 1-15, Nov. 2017.